10-1-2022

Bi-substituted ferrite garnet type magneto-optic materials studied at ESRI nano-fabrication laboratories, ECU, Australia

Mohammad Nur-E-Alam
Edith Cowan University

Mikhail Vasiliev

Kamal Alameh

10.3390/coatings12101471
Nur-E-Alam, M., Vasiliev, M., & Alameh, K. (2022). Bi-substituted ferrite garnet type magneto-optic materials studied at ESRI nano-fabrication laboratories, ECU, Australia. Coatings, 12(10), 1471. https://doi.org/10.3390/coatings12101471

coatings

MDPI

Review

Bi-Substituted Ferrite Garnet Type Magneto-Optic Materials Studied at ESRI Nano-Fabrication Laboratories, ECU, Australia

Mohammad Nur-E-Alam [1,*], Mikhail Vasiliev [2] and Kamal Alameh [3]

[1] School of Science, Edith Cowan University, 270 Joondalup Drive, Joondalup, WA 6027, Australia
[2] ClearVue Technologies Limited, Unit 7/567 Newcastle St., West Perth, WA 6005, Australia
[3] Alpha Solar Tech, Kewdale, WA 6105, Australia
* Correspondence: m.nur-e-alam@ecu.edu.au

Abstract: Since 2007, at the Electron Science Research Institute (ESRI) nano-fabrication laboratories, Edith Cowan University, Australia, we have devoted research efforts to the synthesis and characterization of bismuth-containing ferrite-garnet-type thin-film magneto-optic (MO) materials of different compositions. We report on the growth and characteristics of radio frequency (RF) magnetron sputtered bismuth-substituted iron-garnet thin films. We study the process parameters associated with the RF magnetron sputter deposition technique and investigate the results of optimizing process parameters. To achieve the best MO properties, we employ a few unique techniques, such as co-sputtered nanocomposite films and all-garnet multilayer structures, as well as the application of oxygen plasma treatment to amorphous garnet layers immediately following the deposition process. We demonstrated a remarkable enhancement in the MO properties of Bi-containing ferrite-type garnet thin-film materials, including record-high MO figures of merit and improved conventional and unconventional hysteresis loops of Faraday rotation. Previously unpublished research results on the forward-looking applications of magnetic garnet coatings applied to microparticles of advanced luminescent materials are reported. In the context of developing the next-generation ultra-fast optoelectronic devices, such as light intensity switches and modulators, high-speed flat panel displays, and high-sensitivity sensors, it is important to consider the desirable optical, magnetic, and magneto-optic properties that are found in highly bismuth-substituted iron garnet thin-film materials of various composition types.

Keywords: Bi-substituted; RF magnetron; sputtering; annealing; oxygen plasma treatment; magneto-optic; Faraday rotation; figure of merit; hysteresis loop; imaging; sensing

Citation: Nur-E-Alam, M.; Vasiliev, M.; Alameh, K. Bi-Substituted Ferrite Garnet Type Magneto-Optic Materials Studied at ESRI Nano-Fabrication Laboratories, ECU, Australia. *Coatings* **2022**, *12*, 1471. https://doi.org/10.3390/coatings12101471

Academic Editor: Alexandre Botas

Received: 31 August 2022
Accepted: 29 September 2022
Published: 5 October 2022

1. Introduction

Substitution of bismuth into iron-based garnets enhances the magnetic properties of garnet thin films and monocrystals. Since 1960, after the first discovery of the extraordinary optical and MO properties of garnet thin-film materials, up until today, many researchers worldwide have been devoting efforts to exploring various composition types of garnets and their composition-dependent properties, which are also governed by the garnet layer fabrication technology and related processes [1–7]. The exceptional optical and magneto-optical properties in the near-infrared spectral region make the bismuth-substituted iron garnets the most promising magneto-optical dielectric ferrimagnetic materials [6–10]. However, the practical application of Bi-substituted iron garnets in the visible and short-wavelength infrared parts of the spectrum remains limited due to high optical absorption (especially in sputtered films) in these spectral regions [11–15]. Moreover, the most developed practical uses of garnet materials are in MO imaging and sensing [14–19]. Achieving further improved garnet material properties to suit an expanding variety of applications, as well as future progress in technological and component-level advances, are still required. New material system development is likely to be the source of these enhancements. MO thin-film garnet materials (of both the single and multilayer types)

and nano-structured magnetic photonic crystals (MPCs) have emerged as a cutting-edge research area worldwide [20–30]. Fabrication of high-quality thin films with strong control over their microstructure, surface and interface quality, and optical and magnetic behaviors is required for the successful practical deployment of these garnet materials. The use of RF magnetron sputtering allows for fine control of thin film deposition process parameters, ensuring the production of high-quality thin films and multilayers [12,13,31–37]. Sputtering deposition technology also provides large-area scalability in manufacturing of integrated components requiring advanced functional materials.

In this article, we have monographed our last twelve years of study in the field of Bi-containing ferrite-type garnet materials. We explored the techniques for altering the microstructure of thin films and the ways in which garnet crystals are formed. Some of the material system development results we demonstrated confirm the suitability of several new types and classes of nanocrystalline garnet films for a diverse array of applications including security and digital forensics, biomedical imaging, signal processing, and high-speed optical data processing in communications systems.

2. Materials Composition Studied, Garnet Development Approaches, Technological Processes, and Characterization Techniques

2.1. Materials Composition Studied and Multilayer Structures

We have investigated a range of Bi-containing metal-doped iron garnet materials. Table 1 lists the material composition types, the focus areas of each study, the development approaches used, and the publications resulting from our studies.

Table 1. Types of materials composition, study focus, methodologies used, and the best (highest) obtained specific Faraday rotations in the visible region.

Material Composition Type and Multilayer Structures	Focus of Studies	Methodology	Specific Faraday Rotation (°/μm) in the Visible Wavelength Range		Major Publication
			532 nm	635 nm	
$(Bi,Dy)_3(Fe,Ga)_5O_{12}$: Bi_2O_3	The focus was to investigate the effects of additional extra bismuth oxide content that can lead to significant improvements in the optical transparency and specific Faraday rotation of sputtered garnet materials in the visible range.	Co-sputtering	9.8	2.6	Optics Express, DOI:10.1364/OE.17.019519 [12]
$Bi_{2.1}Dy_{0.9}Fe_{4.3}Ga_{0.7}O_{12}$	The motivation was to explore a new garnet-film stoichiometry type, which was expected to possess somewhat "intermediate" magnetic anisotropy properties, i.e., having neither the in plane nor perpendicular magnetization direction.	Sputtering	10.12	1.66	Optical Materials Express, DOI:10.1364/OME.7.000676 [37]
$Bi_3Fe_5O_{12}$:Dy_2O_3	$Bi_3Fe_5O_{12}$: Dy_2O_3 (between 2.7 and 20 vol. % of added dysprosium oxide content) garnet-type nanocomposite thin-films have been prepared to synthesize a garnet material with the highest possible bismuth substitution level approaching 3 formula units and to obtain the best possible MO properties, even though the thin garnet layers sputtered from a ceramic stoichiometrically mixed oxide-based $Bi_3Fe_5O_{12}$ target unexpectedly showed negligible Faraday rotation.	Co-sputtering	13.30	3.23	Optical Materials Express, DOI:10.1364/OME.4.001866 [31]
$Bi_{1.8}Lu_{1.2}Fe_{3.6}Al_{1.4}O_{12}$: Bi_2O_3	This study focused on the fabrication of RF sputtered $Bi_{1.8}Lu_{1.2}Fe_{3.6}Al_{1.4}O_{12}$ and the results of adjusting the optical and magnetic properties of these films utilizing co-sputtering deposition using an additional bismuth oxide target.	Co-sputtering	6.25	1.99	Optical Materials Express, DOI:10.1364/OME.1.000413 [35]

Table 1. *Cont.*

Material Composition Type and Multilayer Structures	Focus of Studies	Methodology	Specific Faraday Rotation (°/μm) in the Visible Wavelength Range		Major Publication
			532 nm	635 nm	
$Bi_2Dy_1Fe_4Ga_1O_{12}$: $Bi_3Fe_5O_{12}$	The co-deposited all-garnet garnet-mix-type films were synthesized to obtain the ultimate (highest possible) bismuth substitution level without using a single-target $Bi_3Fe_5O_{12}$ sputtering process (which was found to result in films not crystallizing into garnet phase unless composition-diluted through co-sputtering).	Co-sputtering	8.25	1.52	Procedia Engineering, 76 (2014), 61-73. DOI: 10.1016/j.proeng.2013.09.248 [34]
$Bi_{0.9}Lu_{1.85}Y_{0.25}$ $Fe_{4.0}Ga_1O_{12}$	The motivation was to explore a new type of garnet material stoichiometry, ($Bi_{0.9}Lu_{1.85}Y_{0.25}Fe_{4.0}Ga_1O_{12}$), with a combined substitution of Bi and Lu ions at yttrium (Y) lattice sites, which has so far not been explored extensively using physical vapor deposition techniques. Special attention was devoted to the synthesis of a garnet layer with its lattice parameter as close as possible to that of $Y_3Fe_5O_{12}$ (YIG), and to obtaining low coercivity for applications requiring magnetization-state switching such as MO imaging.	Sputtering	1.25	0.89	Nanomaterials, DOI: 10.3390/nano8050355 [36]
All-garnet multilayer structures	The goal was to explore the engineering of magnetic properties in garnet multilayers, and especially to identify the ways of adjusting the coercive force and magnetic switching and magnetic anisotropy properties by varying the component layer stoichiometries. The effects of exchange coupling on magnetic switching properties of all-garnet multilayer thin film structures have been studied in detail.	Sequential sputtering	NA		Materials 2015, 8, 1976-1992; DOI:10.3390/ma8041976 [32]
Garnet layer/oxide layer structures	A new technological approach has been applied for the RF-magnetron sputter deposition and annealing crystallization of Bi-substituted iron garnet films.	Sequential sputtering	~2.7 times increment of MO quality factor obtained in crystallized films.		Materials 2020, 13, 5113; DOI:10.3390/ma13225113 [33]

We have applied different techniques to deposit garnet layers by using the RF magnetron sputtering technique including co-sputtering (using garnet and oxide targets and pairs of dissimilar garnet-stoichiometry targets), the sequential sputtering technique for multilayer garnet structures, garnet layers deposited under protective oxide layer, and post-deposition oxygen plasma treatment. After the deposition process, all as-deposited thin-film layers were subjected to a conventional oven annealing processes (which were developed and optimized separately for each of the garnet material types synthesized). The composition-dependent annealing crystallization regimes (crystallization time, process temperatures and temperature-ramping rates) were found by multiple trials and sometimes by designing multi-step reannealing processes. The modified techniques used to prepare the garnet layers in our study are described in the following subsections.

2.2. RF Magnetron Sputtering and Co-Sputtering Processes

Using RF magnetron sputtering and co-sputtering technique (as schematically shown in Figure 1) in low-pressure (1–2 mTorr) pure argon plasma atmosphere without additional oxygen input, bismuth-substituted iron garnet and composite-type films were fabricated on glass (Corning 1737) and monocrystalline gadolinium gallium garnet (GGG) substrates. The deposition rates were observed during sputtering processes by using a well-calibrated quartz crystal microbalance sensor to monitor the film thickness. For the composite films, the estimated amounts of the volumetric fraction of additional components (of either garnet or oxide type) were calculated from the measured partial deposition rates from both sputtering targets (base garnet target and other targets). The basic formula that was used to calculate the vol.% fraction of excess additional components (oxides or garnet) for the composite-type layers is described in Refs. [12,13]. We studied several types

of garnet-oxides and all-garnets composite films and reported their best-achieved MO properties [12,31,35,37].

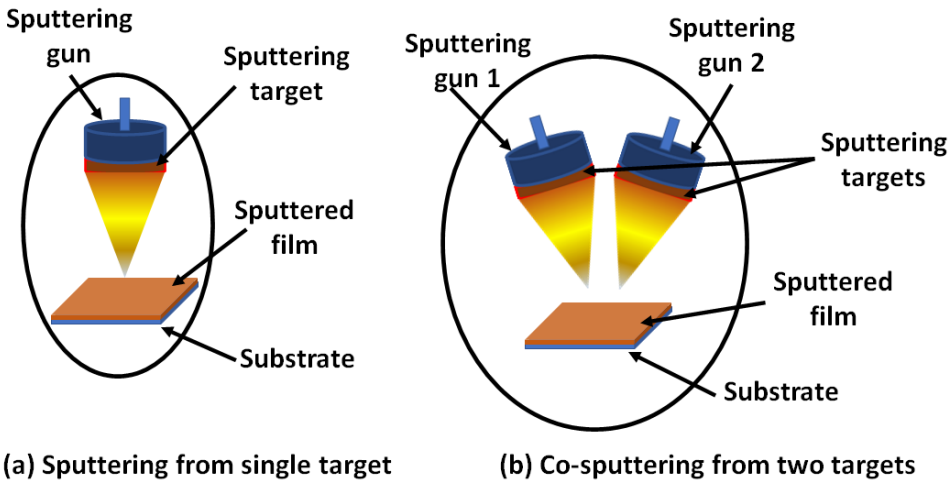

Figure 1. Schematic diagram of RF magnetron sputtering and co-sputtering techniques used for garnet and composite layers fabrication.

The detailed garnet materials development and characterization results, including some unconventional magnetic properties found in all-garnet multilayer systems and the proposed new forward-looking applications of magnetic garnet films deposited onto surfaces of luminescent material particles are described in the following sections.

2.3. Sequential Sputtering of Multilayer Garnet Structures

Figure 2 shows the schematic diagram of the sequential sputtering process that is used to deposit all-garnet multilayer structures including the material composition types and their magnetic behaviors. The various layer material combinations in all-garnet multilayer structures were created using the optimized deposition techniques and an RF magnetron sputtering system. A layer of magneto-soft, low-coercivity material was sandwiched between two magneto-hard layers with high uniaxial magnetic anisotropy and constant thickness inside the multilayer constructions. A sequential sputtering process was used to deposit all-garnet multilayer structures with various garnet-type materials and layer thicknesses (i.e., a single deposition run of each layer using oxide mix-based ceramic sputtering targets and at low-pressure pure-argon plasma). The process parameters, conditions, and optimization of annealing regimes to prepare all-garnet multilayers structures obtaining very smooth layer interfaces, defect-free microstructure morphologies, and microcrack-free surfaces are detailed in Ref. [32].

Even though the sequential sputtering of dielectric material layers is a conventional technology, we identified some unconventional (and initially unexpected) magnetic behaviors in tri-layer exchange-coupled garnet systems made using materials of different magnetic anisotropy types.

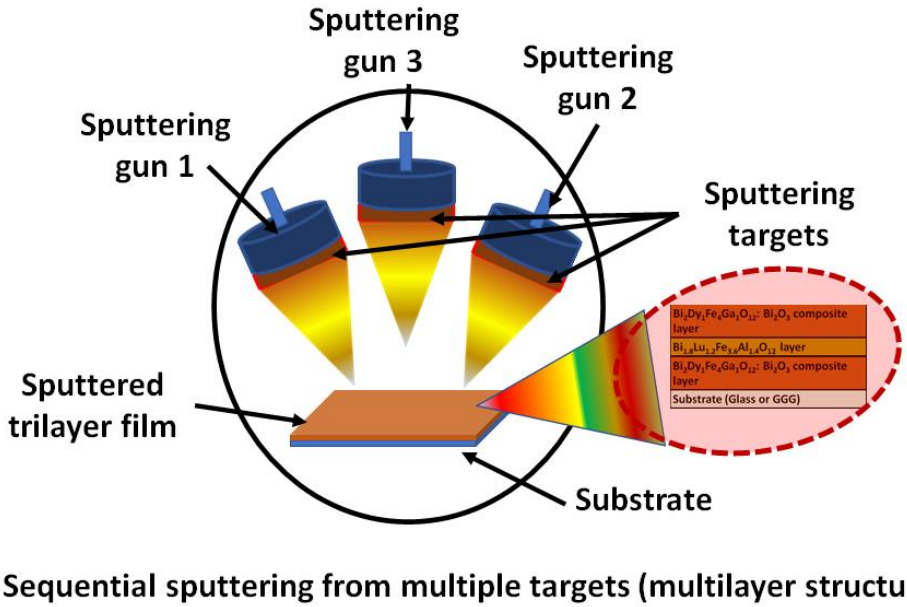

Figure 2. Schematic diagram of the sequential sputtering technique used to deposit the all-garnet multilayer structures.

2.4. Garnet Layer Formed under a Protective Oxide Layer

To enhance the qualities of highly Bi-substituted iron garnet thin film materials, completely new and improved process sequences for annealing crystallization of garnet thin films were investigated. A protective layer of bismuth oxide (Bi_2O_3) that is only slightly thicker than the garnet layer (2–20 nm) is necessary to produce high-performance ultrathin garnet films because it helps the garnet layer become crystallized while reducing the loss of bismuth substitution content. In the beginning, a GGG or glass substrate was coated with a 20–60 nm amorphous-phase layer made of the nanocomposite co–sputtering material type ($Bi_2Dy_1Fe_4Ga_1O_{12}$ + 10–40 vol.% of Bi_2O_3). In the second process stage, a protective bismuth-oxide layer of thickness between 2 nm and 20 nm was deposited by using RF magnetron sputtering onto the amorphous nanocomposite films (as schematically presented in Figure 3) before running the annealing crystallization in an air atmosphere, at a (composition-dependent) temperature between 490 °C and 650 °C [33]. Results of the demonstrated garnet layer development are summarized in the next section.

2.5. Post-Deposition Oxygen Plasma Treatment Applied to As-Deposited Garnet Layer

The oxygen plasma treatment of as-deposited garnet film samples was applied immediately after the deposition. We investigated the effects of post-deposition oxygen plasma treatment on the MO properties of RF sputtered garnet thin-film layers, synthesized using two different types of Bi-substituted garnets. Figure 4 shows the schematic diagram of the flow chart used for post-deposition oxygen plasma treatment of amorphous garnet layers.

The oxygen plasma treatment was conducted using YZD08-5C plasma cleaner (purchased through Alibaba.com) for 0.5–5 min. Oxygen plasma-treated films (after annealing crystallization) showed better film quality and properties (specific Faraday rotation and MO figure of merit at 532 nm) than those of the non-treated samples [33]. In addition to all these modified techniques used to deposit garnet and multilayer structures for the improvement and property enhancement of garnet layers in terms of their optical and magneto-optical properties, we also studied and investigated the influence of varying deposition process parameters and the corresponding effects on the garnet layer growth and their properties measured after annealing crystallization as described in Section 2.6.

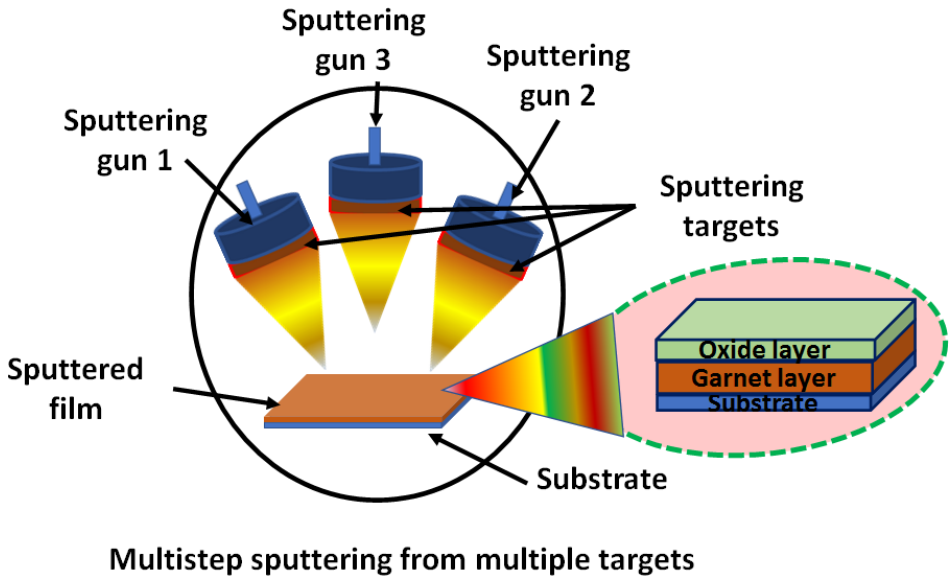

Figure 3. Schematic diagram of a multistep sputtering technique used for garnet/oxide multilayer (garnet layer under protective layer) structures deposition.

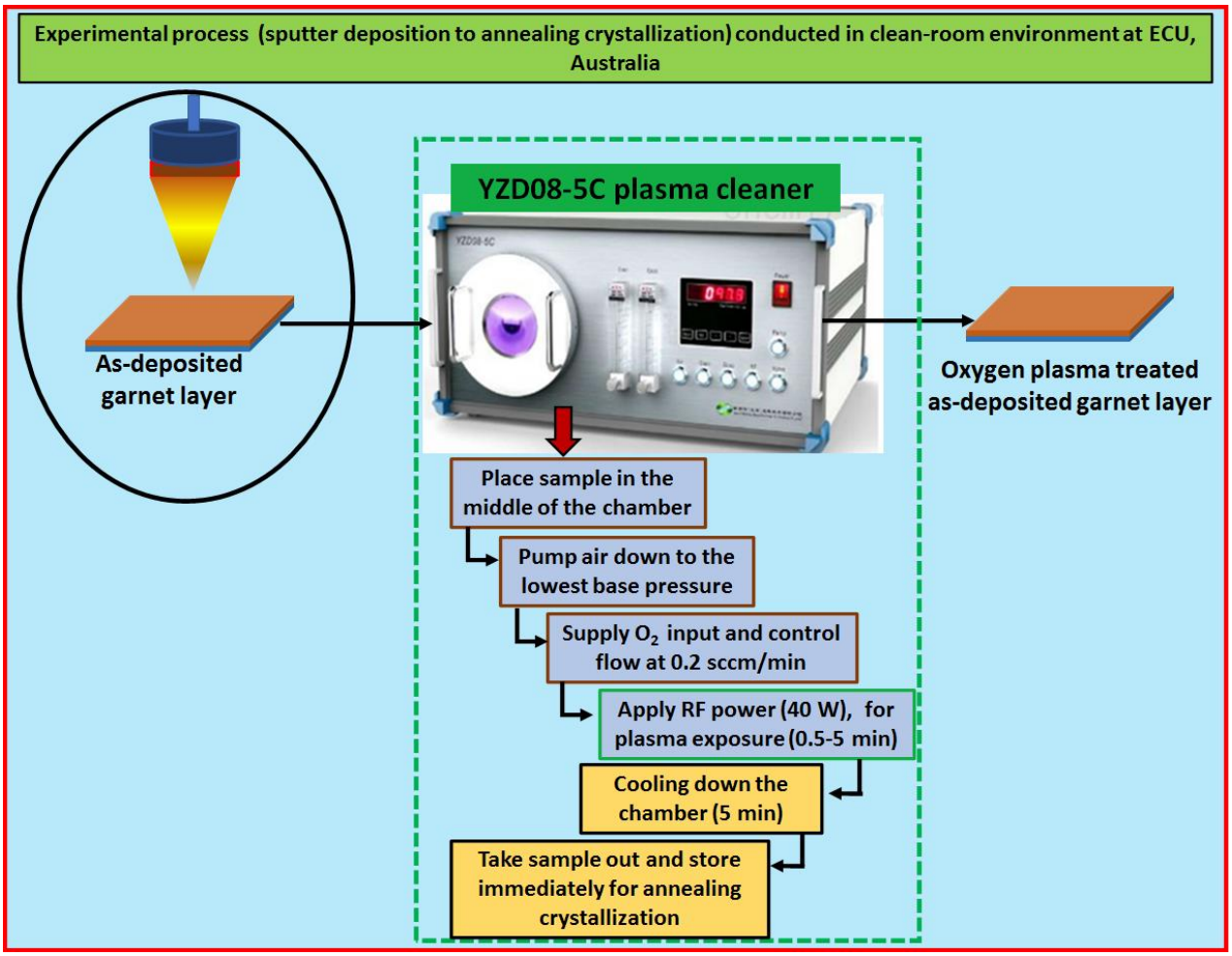

Figure 4. Schematic diagram of the flow chart of oxygen plasma treatment process applied to as-deposited garnet layers.

2.6. Investigation of Deposition Process Parameter Effects on Garnet Layers

We investigated the influence of RF magnetron sputtering process parameters on the magneto-optical (MO) characteristics of heavily bismuth-substituted ferrite garnet films of composition type $Bi_{2.1}Dy_{0.9}Fe_{3.9}Ga_{1.1}O_{12}$. The variations in RF sputtering process parameters (substrate stage temperature and rotation rate) influence the properties (films' stoichiometry and MO quality through variations in both the specific Faraday rotation and the optical absorption coefficients) of garnet films. We concluded from this study that the MO characteristics can be tuned and optimized for use in various magnetic field-driven nano-photonics and integrated optics devices with the addition of a flexible and economical approach for the design and development of new, high-quality, and application-specific MO materials for various photonics and integrated-optics applications [38].

2.7. Preparation of Garnet-Coated Magnetic Fluorescent Micro/Nanoparticles

We prepared garnet-coated magnetic fluorescent micro/nanoparticles by using a finely ground powder of an upconversion-type luminescent material (a rare-earth-ion doped rare earth oxide-based luminophore material of generic formula type Re_2O_3), and a highly bismuth-substituted ferrite garnet material target of composition type $Bi_{2.1}Dy_{0.9}Fe_{3.9}Ga_{1.1}O_{12}$. We sputtered the garnet layer on top of a partially agglomerated (sub-mm thick) layer of fluorescent particles placed over the surface of a substrate holder inside a sputtering system. A schematic diagram of the multifunctional material synthesis process can be seen in Figure 5. In the first stage, we mixed the ground Re_2O_3 powder with a small amount of isopropanol on a glass substrate and made a thin layer of agglomerated (clay-like) powder mixture. Once the isopropanol evaporated in the ambient air atmosphere, the powder became dry and essentially formed a clay-coated glass substrate which was then placed into a RF magnetron sputtering chamber for the subsequent deposition of the garnet-stoichiometry layer. Around 100 nm of garnet layer thickness (as gauged by a calibrated quartz microbalance sensor) was deposited from the above-mentioned sputtering target using the well-known sputter deposition process parameters that we have developed for this garnet composition during our previous work. After the sputtering deposition, the garnet-coated "clay" layer was subjected to high-temperature annealing (annealed in air at 630 °C for approx. 2 h) process. The annealing process enabled the crystallization of the top garnet-coated part of the combined material system that was seeded on top of the fluorescent microparticle layer. The annealed garnet-coated fluorescent material layer was removed from the glass substrates and ground to convert into small particles (mean particle size of near 15 microns). As can be seen from Figure 5, the very last image of the schematic diagram shows the practically achieved multifunctional magnetic-fluorescent micro/nanoparticles. This study is still in its preliminary stages to make any detailed scientific reports; however, we believe that these magnetic fluorescent microparticles (possessing high remnant magnetization and responsive to external stimulation by externally applied magnetic fields, e.g., see the video in the Supplementary Section) can be potentially useful for many future biomedical imaging applications, including cancer cell detection, labeling, and even their possible manipulation/removal from blood vessels, by way of magnetic field-driven manipulation (similar experiments with biological cell manipulation using ferromagnetic particles, but without intinsic fluorescent labeling by the same particles have been reported in Ref. [39]). A short video of magnetized magnetically manipulated multifunctional fluorescent micro/nanoparticles movement is supplied in the Supplementary Section of this manuscript.

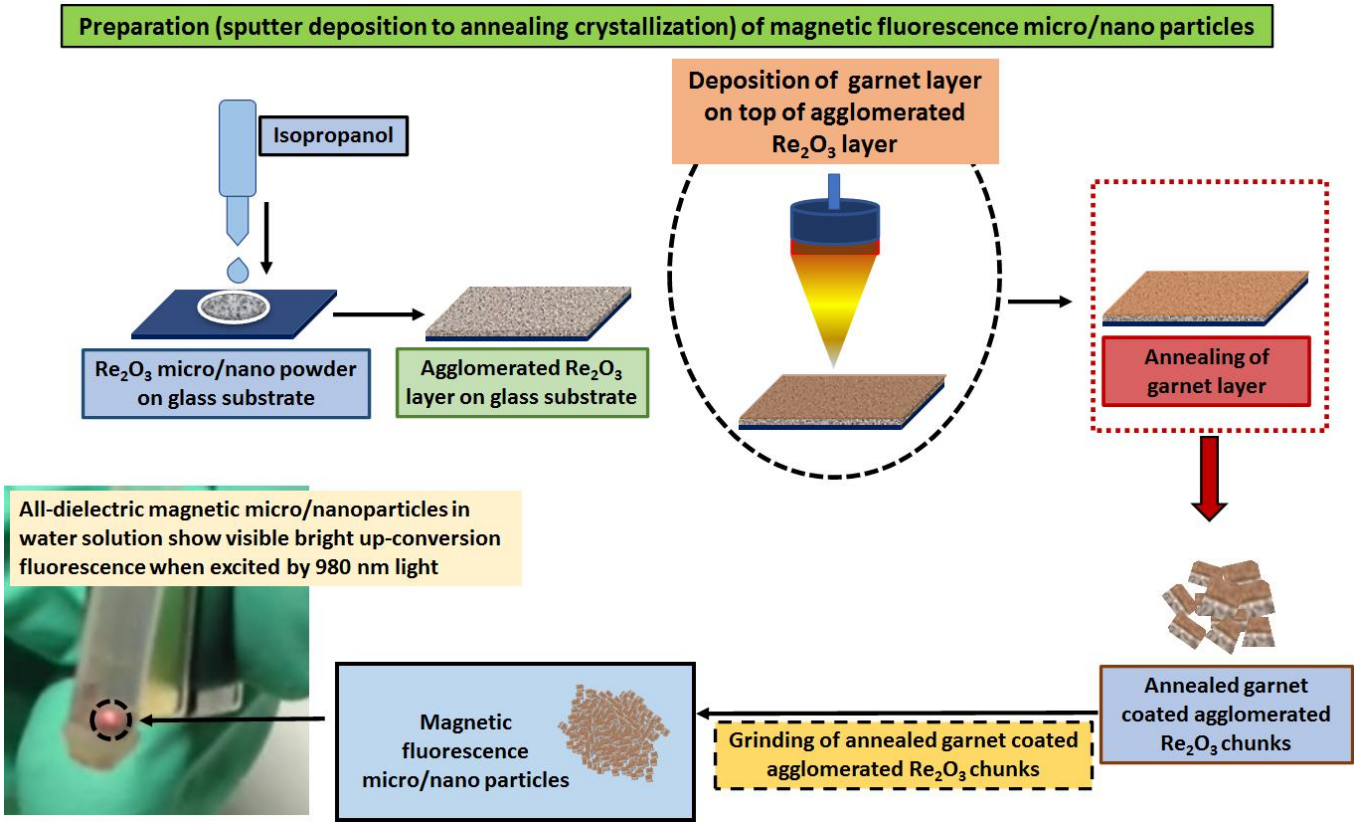

Figure 5. Schematic representation of magnetic fluorescent micro/nanoparticles preparation process.

A feature of particular interest for the possible future biomedical (and possibly also other) applications of these fluorescent-magnetic multifunctional microparticles enabled by our group's research into magnetic garnet coatings is related to the high visible-range transparency of thin garnet coatings possessing high uniaxial magnetic anisotropy (and high remnant magnetization), allowing the visible (red) luminescent emissions to escape from under the garnet coating, remaining sufficiently bright. In our experiments, the luminescence excitation source was a (50 mW) 980 nm IR laser, and the red luminescent emissions were of upconversion type. Despite the relatively small amounts of the optical power emitted by particles (or particle agglomerates), they remained brightly visible due to the high visible-range transmission of garnet coatings covering the fluorescent microparticles. To the best of our knowledge, no similar experiments with microparticles of advanced luminescent materials coated with any sputtered magnetic garnet layers of similar composition types have been reported so far.

2.8. Annealing Crystallization Processes and Material Characterization Techniques

All the as-deposited garnet layers or multilayer structures were subjected to oven annealing at high temperatures, as the after-deposited garnet layers remain in amorphous phase and show no magnetic or MO properties even if sputtered at high substrate temperatures (up to about 700 °C, in our group's experience). A conventional temperature/ramp-controlled box furnace oven was used to anneal the as-deposited (amorphous) garnet layers in the air atmosphere. The post-deposition annealing treatment allows the softening of the materials, enables the inter-diffusion of metal-oxide precursors, and simultaneously leads (on achieving the necessarily high crystallization process temperature) to the desired changes in the microstructure and other properties of the sputtered garnet layers. The annealing heat treatment of thin films is a sequence of three distinct process steps, including a temperature ramp-up process, holding the specified suitable temperature for a distinct time for isothermal crystallization, and cooling down-ramp at the same or at a different

rate compared to the ramp-up rate as can be seen in Figure 6a. It is found that composition substantially influences the annealing regimes (temperature and duration) optimization. The amorphous (as-deposited) layers were crystallized into a high-quality nanocrystalline garnet phase with relatively small grain sizes using an annealing procedure lasting 1 to 10 h, depending on the type of garnet composition (tens of nm). Since high-temperature ramp rates or even rapid thermal annealing (RTA) were found to cause microcracks and surface damage in garnet layers, moderate temperature ramp rates (comparatively low ramp rates) were recommended to crystallize the amorphous garnet layers [40]. However, we have noticed that for some compositions lower cooling down-ramp is the better option to get crystallization of the garnet layer. In addition, we studied the annealing behavior and the crystallization kinetics of garnet-Bi_2O_3 composite films that yielded the estimates of the activation energy of isothermal crystallization for this type of material resulting in a guide for obtaining high-performance garnet films and for the design of optimized thermal processing regimes suitable for the synthesis of highly Bi-substituted garnets using physical vapor deposition methods [41]. As schematically shown in Figure 6a, the annealing process optimization experiments carried out to find the most suitable annealing regimes (in terms of both the maximum process temperature and crystallization process duration) for the garnet layers and multilayer structures can be used as a guide to establish the optimized annealing regimes for virtually any garnet or non-garnet film layers.

The microstructure, optical, magnetic, and MO properties of optimally annealed and high-quality garnet and composite type garnet thin films were examined. We analyzed the X-ray diffractometry (XRD) and energy-dispersive X-ray spectroscopy (EDS) data to determine the crystal structure and impurity phases. A UV/Visible spectrophotometer was used to measure the transmission spectra, and the absorption co-efficient spectra were then derived to learn more about the optical properties of garnet films. Later, using a combination of custom-built spectrum-fitting software and Swanepoel's envelope method to get around the spectral constraints of our previous measurement method, we accurately determined the optical constants data for multiple rare-earth doped iron garnets simultaneously with the garnet film thicknesses from the optical transmission spectra. This method helped us overcome the limitations of our previous measurement method with respect to spectral range [42]. The magnetic and MO properties of the garnet films were characterized by measuring the Faraday rotation angle (almost across the entire visible spectral region) and Faraday rotation hysteresis loops. The experimental set-up for measuring the optical transmission and specific Faraday rotation is schematically detailed in Figure 6b,c. Other than these characterizations, we performed the magnetic circular dichroism (MCD) measurements for some garnet material composition types with the help of our international research collaborators in the Russian Federation (Prof. V.A. Kotov's Group at the Institute of Radio Engineering and Electronics, Moscow).

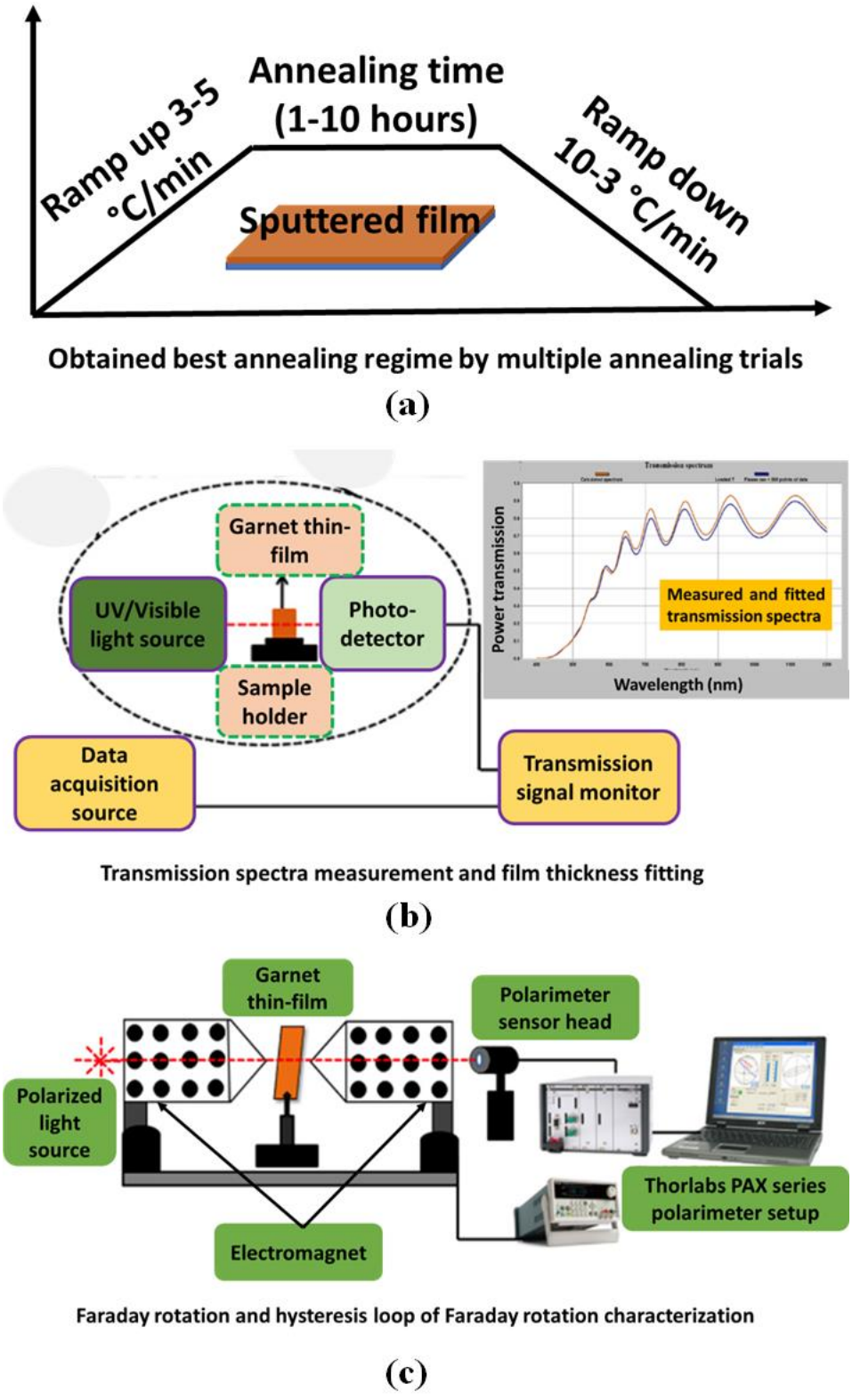

Figure 6. Schematic diagram of the annealing crystallization process of garnet layer (**a**), measurement of optical transmission spectra to derive the film thickness and absorption coefficient (**b**), and specific Faraday rotation and hysteresis loop of Faraday rotation characterization methodologies (**c**) [13].

3. Results and Discussion

A range of MO garnet and composite layer material types (garnet-oxide, garnet-garnet, and multilayer structures) materials with high bismuth content were synthesized, char-

acterized, studied, and evaluated in terms of the optical, and magneto-optical properties. In this section, we would like to present a glimpse of the best achieved optical and MO properties that we have observed and reported in multiple scientific publications. Figure 7 presents an example of obtained optical and MO properties of garnet layers prepared by various development approaches, e.g., synthesizing the garnet-oxides composites, applying post-deposition oxygen plasma treatment, and garnet layers deposited using different substrate stage rotation rates (rpm).

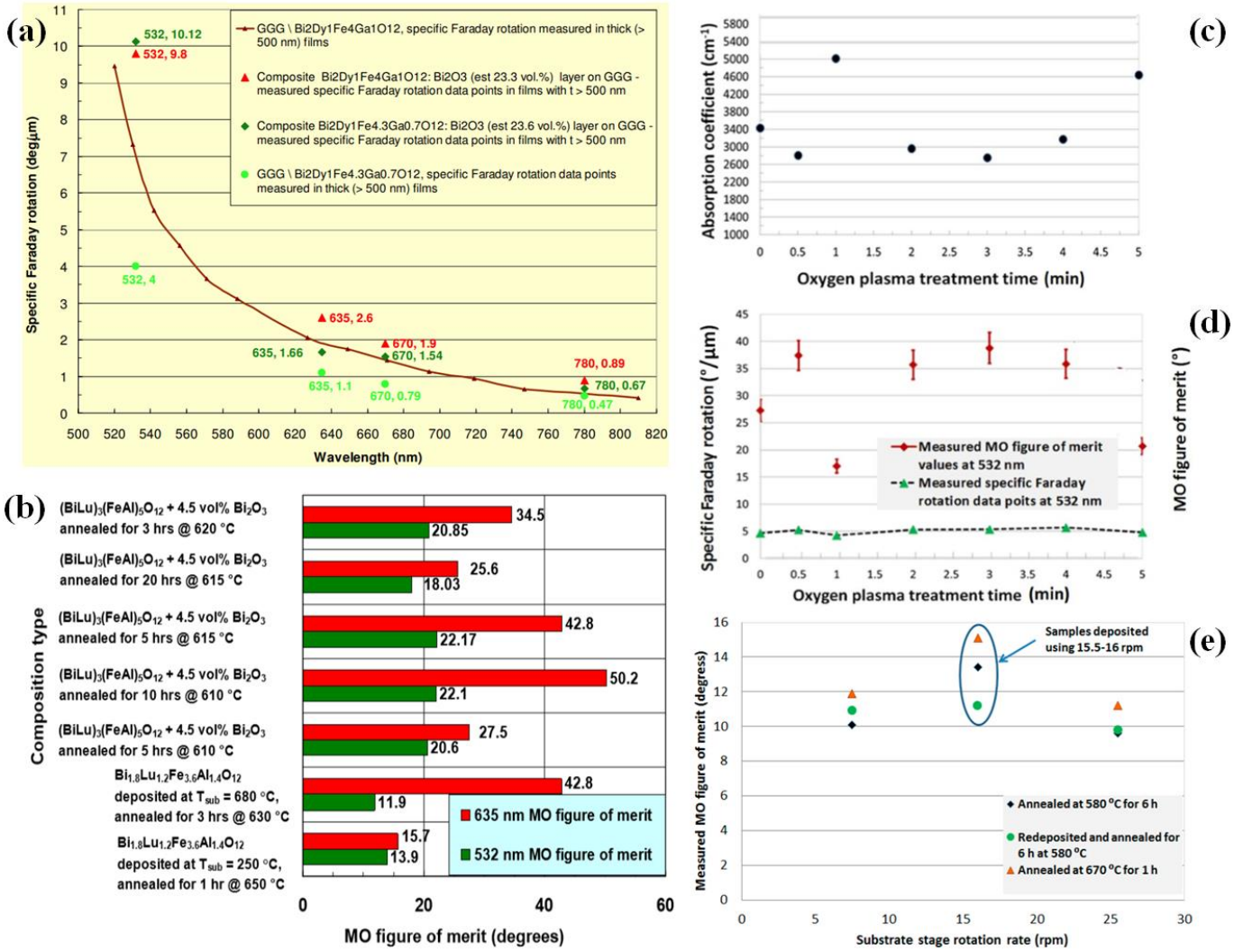

Figure 7. Optimized (best achieved by our group so far) optical and MO properties observed on garnet layers prepared by different development approaches. The best obtained specific Faraday rotation of garnet films ($Bi_2Dy_1Fe_4Ga_1O_{12}$), presented with the measured specific Faraday rotation data points achieved in $Bi_2Dy_1Fe_{4.3}Ga_{0.7}O_{12}$ garnet films and the best performing garnet-Bi_2O_3 composite films (**a**), measured MO quality factor in terms of the figure of merit of typical $Bi_{1.8}Lu_{1.2}Fe_{3.6}Al_{1.4}O_{12}$ garnet layer and deposited at 250 °C and 680 °C substrate temperature and several best annealed composite $Bi_{1.8}Lu_{1.2}Fe_{3.6}Al_{1.4}O_{12}$: (4.5 vol. % Bi_2O_3) films (**b**), improved optical and MO properties observed in oxygen plasma treated garnet films, and the garnet layers deposited using various substrate stage rotation rates (rpm) [13,33,37,38].

The obtained material characterization results indicate that the MO properties across the visible spectral range can be significantly improved in composites possessing an excess of co-sputtered components (metal oxides, or metal doped garnets). When compared to epitaxially grown (LPE) garnet monocrystals, polycrystalline sputtered garnet-composite

layers exhibit higher optical absorption. The optical transparency of sputtered garnet materials can be significantly improved by the addition of other components (such as bismuth oxide, dysprosium oxide, and others) in order to decrease optical absorption and boost specific Faraday rotation in the visible range. High specific Faraday rotation (which confirms high Bi substitution levels attained) or low optical absorbance across a large portion of the visible spectrum range were found to characterize the best-annealed high-quality garnet-composite thin films. The highest-quality garnet-composite thin films that had been appropriately annealed showed either high specific Faraday rotation (which confirmed the high Bi substitution levels attained) or low optical absorption across large parts of the visible spectral range. Higher transparency across the near-infrared range and significantly lower absorption coefficients across the visible spectral region compared to the garnet layers sputtered using conventional methodologies confirms the hypothesis of developing high-quality nanocomposite oxide-mixed garnet layers for various existing and forward-looking MO applications including sensing and imaging [12,13,31,34]. We obtained improved materials properties in sputtered garnet films, whereas there was limited progress made at the same time in LPE and some progress reported in pulsed laser deposited (PLD) films, as can be seen in Table 2, that record high MO quality factors in the visible spectral range achieved in sputtered films. However, each of the garnet material's stoichiometry and their combined properties are unique and not directly comparable with each other. Bi-substituted garnet-type materials' MO characteristics are entirely composition-dependent, making them also application-specific. Bi-substituted iron garnets and composites have been synthesized and characterized using numerous research projects to acquire the optimum material properties suited for a variety of applications, including microwave-range, communication band-wavelength, and integrated photonics applications [43–47].

Table 2. List of Bi-substituted iron garnet materials with their corresponding measured MO quality factors in the visible spectral range, and their fabrication processes details.

Materials Short Name	Materials Nominal Stoichiometry	Obtained Figure of Merit at 532 nm (°)	Fabrication Process
BIG	$Bi_3Fe_5O_{12}$	9.0 ± 0.5	PLD [48]
BIGG	$Bi_3Fe_4Ga_1O_{12}$	16.5 ± 1.0	PLD [48]
BiDyIG	NA	6.8	Biased target ion beam deposition (BTIBD) [49]
BiCeDyIG	NA	13.1	BTIBD [49]
$Bi_{2.5}$Ga:NIG	$Nd_{0.5}Bi_{2.5}Fe_{5-y}Ga_yO_{12}$ (Y = 0–1)	<6	Metal organic decomposition (MOD) [50]
$(Bi,Dy)_3(Fe,Ga)_5O_{12}$: Bi_2O_3 composites	NA	29.5	RF magnetron co-sputtering [12]
$Bi_{1.8}Lu_{1.2}Fe_{3.6}Al_{1.4}O_{12}$: Bi_2O_3 composites	NA	22.1	RF magnetron co-sputtering [37]

Figure 8 shows the measured hysteresis loops of various types of garnet-oxide composite films having different volumetric fractions of extra oxide content and multilayer structures.

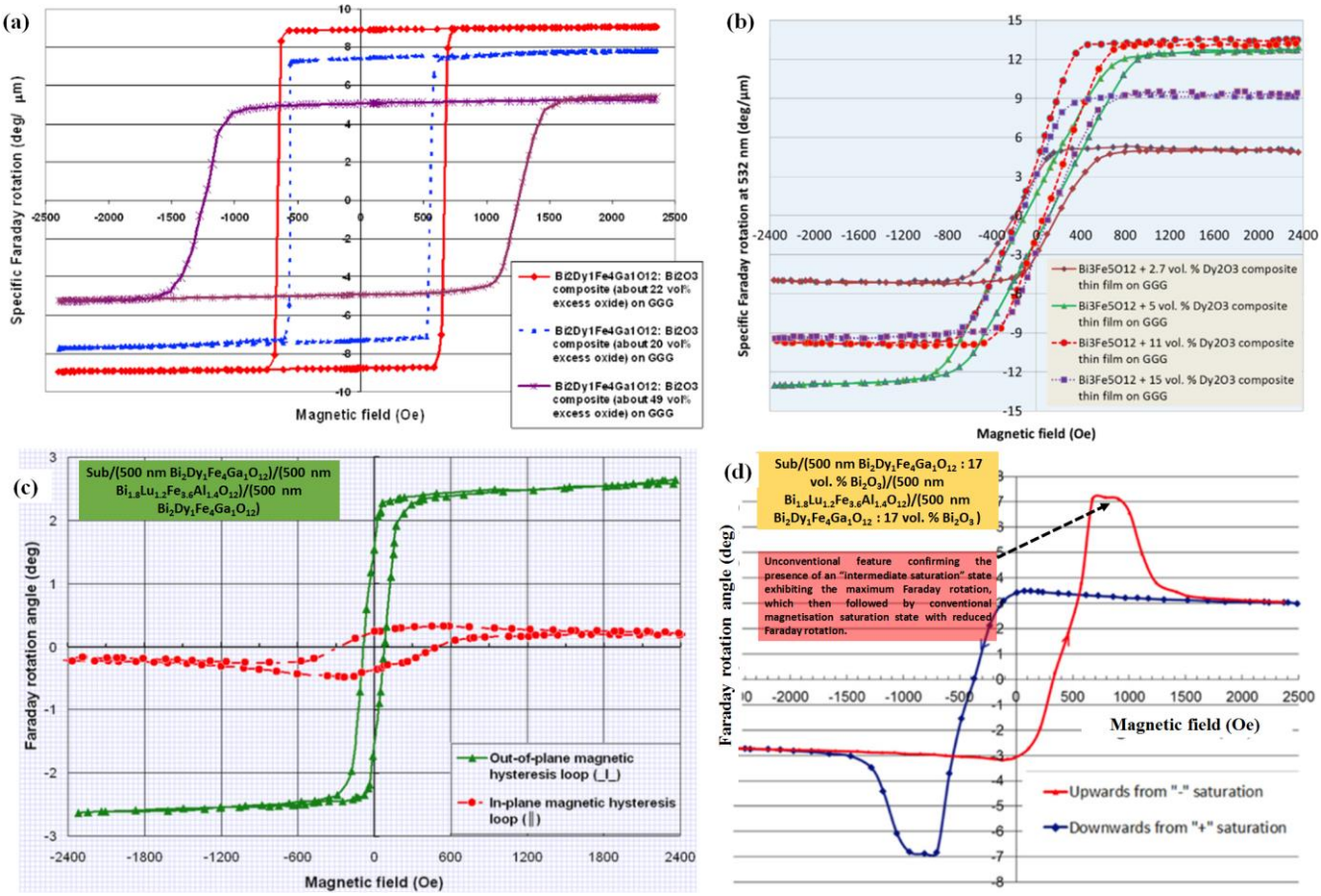

Figure 8. Measured hysteresis loop of Faraday rotation in different types of garnet-oxides composite layers and multilayer structures. The effects of excess oxide content added to the base garnet layers were observed. Measured hysteresis loops of $((Bi,Dy)_3(Fe,Ga)_5O_{12}$: $Bi_2O_3)$ composite films having different volumetric fractions of extra Bi_2O_3 (**a**), $Bi_3Fe_5O_{12}$: Dy_2O_3) (2.7-15 Vol. %) composite thin films prepared on GGG substrates (**b**), obtained hysteresis loops from an optimally annealed all-garnet multilayer structure prepared on a GGG (111) substrate with an external magnetic field applied both in perpendicular direction (out-of-plane, green color curve) and parallel (in-plane, red color curve) with respect to the film plane of the multilayer structure (**c**), and an unconventional magnetic hysteresis loop measured in a modified all-garnet multilayer structure [12,31,32,34].

Various shapes of hysteresis loops of Faraday rotation were observed in our studied all garnet-oxide composites and multilayer structures. The variation and difference of the coercive force and switching field values observed in co-sputtered garnet layers and in different types of all-garnet multilayer structures revealed the possibility of engineering the magnetic characteristics of garnet materials suitable for different ultrafast switching applications or other time-demanding nanotechnological applications. Hysteresis loops of garnet-oxide $((Bi,Dy)_3(Fe,Ga)_5O_{12}$: $Bi_2O_3)$ composite films having different volumetric fractions of extra Bi_2O_3 were found to be practically square-shaped with the tunable coercive force as presented in Figure 8a, while the additional dysprosium oxide (Dy_2O_3) to the base garnet material of composition type ($Bi_3Fe_5O_{12}$) led to obtaining hysteresis loops of specific Faraday rotation with tunable and comparatively lower coercive force and saturation magnetization values very attractive for low-switching-field applications (Figure 8b). These results also indicate possibly achieving a higher number of Bi-atoms substituted per formula unit into the synthesized garnet layers as per the hypothesis made in the published literature [51]. On the other hand, all-garnet multilayer structures using two high-performance, highly-Bi-substituted iron garnet materials with different magnetic behaviors (magnetic anisotropy types, switching fields, and saturation magnetizations)

enable the potential for obtaining custom-engineered magnetic properties that are (to the best of our knowledge) not possible using single-layer garnet thin films (Figure 8c,d). The notable and unexpected characteristics of the hysteresis loop behavior supported the existence of an "intermediate saturation" state with the maximum Faraday rotation, which was followed by a conventional magnetization saturation state with a reduced Faraday rotation at increasing external magnetic fields above about 1 kOe. The final saturated Faraday rotation was observed at near 1.6 kOe, at below 50% of the maximum Faraday rotation angle seen at smaller fields [32]. These exchange-coupled all-garnet multilayer structures have potential for use in several novel applications and cutting-edge future studies. More research to improve control over the magnetic properties in garnet multilayer structures using various combinations of high-performance garnet materials of varied optimum thicknesses as well as stoichiometry types can result in more novel and surprising discoveries. However, all of the various conventional-type shapes of hysteresis loops observed in our sputtered garnet films are quite comparable to the hysteresis loops obtained in different types of garnet films prepared by using different techniques by other research groups [47,51–53].

Figure 9a–e depicts the measured spectral dependences of the magnetic circular dichroism (MCD) of ferrite garnet films, in the spectral range from 250 to 600 nm, and the microstructural properties of garnet layers and the results of post-deposition effects on microstructures of the annealed garnet layers.

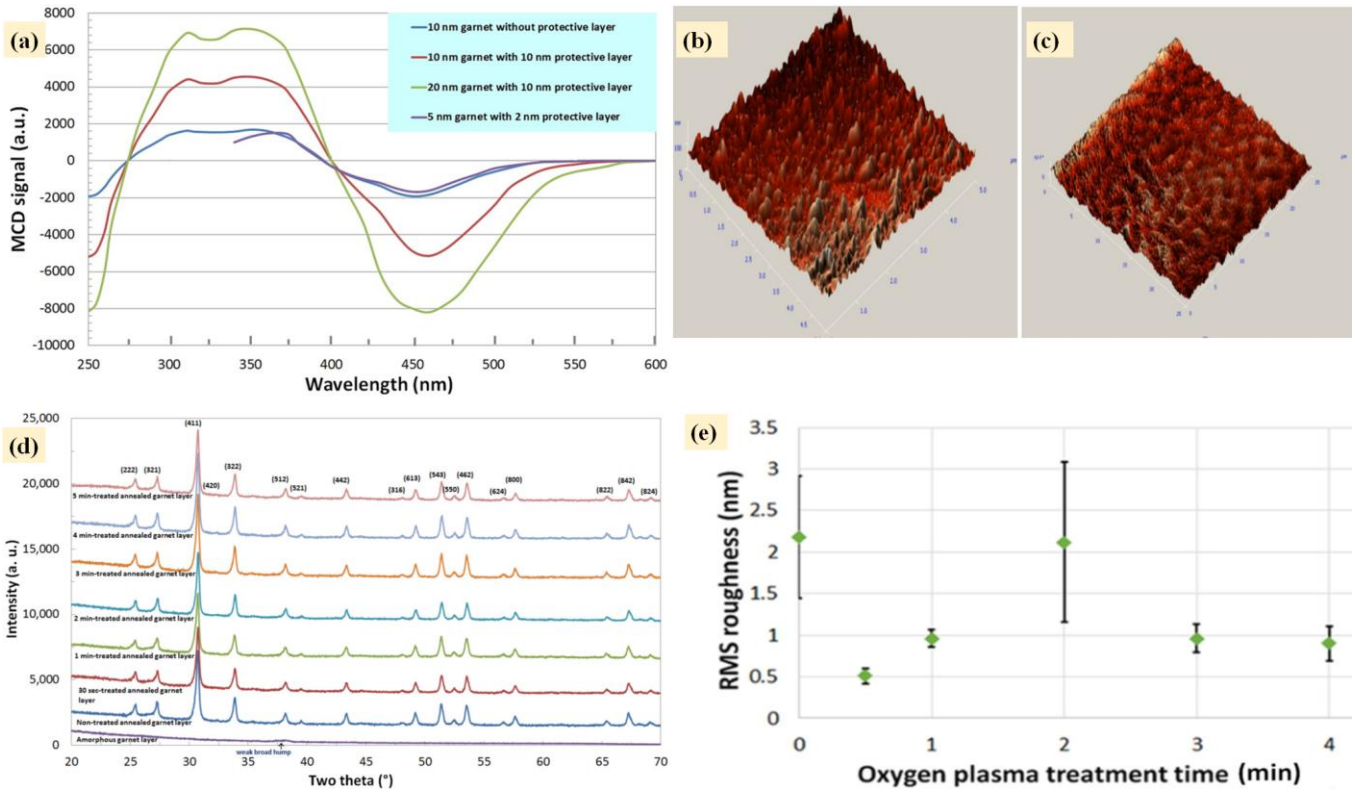

Figure 9. Observed MCD signals from garnet layers prepared under protective layers (**a**), microstructural properties of garnet-oxide composite (**b**,**c**), XRD data, and RMS roughness properties of post-deposition oxygen plasma treated garnet layers followed by optimized annealing crystallization (**d**,**e**) [13,38].

By conducting wavelength-dependent MCD experiments between 250 and 850 nm at ambient temperature and at cryogenic temperatures, it has been determined how thin protective Bi_2O_3 layers affect the MO characteristics of ultrathin, highly bismuth-substituted dysprosium iron garnet layers. An oxide-protected annealed film of the garnet-cover layer system was found to have an MCD signal magnitude that was approximately 2.7 times

greater than an unprotected garnet layer when measured at 450 nm. The MO quality characteristics of garnet thin films were also seen to be significantly superior on garnet layers that underwent oxygen plasma treatment immediately following the deposition process. Plasma treatment could result in better (faster) compensation of oxygen loss occurring during sputtering, preventing the excessive formation of non-garnet material phases during annealing, assuming that pre-diffusion of the oxygen from plasma into garnet film volume occurs before the annealing crystallization process (as can be confirmed from the RMS roughness characterization). Utilizing slightly different or any other accessible garnet film compositions, these effects and procedures still require additional research.

In modern day magneto-optics, rare-earth doped materials play a major role in many areas of integrated optics and photonics applications, including biomedical devices, imaging systems, optical communications networks, and the optical storage media. Magneto-optic garnet materials represent a vast and extensive research area, and it can be quite difficult to present all of the novel developments and this area's results diversity in a single review. However, we believe that Bi-substituted garnet materials developed by our group are suitably aligned with the recently reported roadmap 2022 of current magneto-optics R&D [54,55]. A complete list of our research group publications related to this review article and the study of various garnet materials is also provided in Appendix A, which are not cited in this article.

4. Conclusions

We have extensively investigated and described multiple different approaches to the synthesis of high-quality, highly bismuth-substituted magneto-optic ferrite garnet layers of different composition types not extensively described in the current literature. The various material system development results achieved led to demonstrating the application-specific and highly customizable magnetic and MO characteristics in garnet films and thin magnetic multilayers, which is of interest in various practical application areas, from magnetoplasmonics to the development of multiple sensors, polarization control, and light intensity modulator systems reliant on ultrafast magnetic switching and magnetic field sensitivity.

Supplementary Materials: The following supporting information can be downloaded at: https://www.mdpi.com/article/10.3390/coatings12101471/s1, Video S1: "Magnetic field-induced movement of multifunctional upconverting fluorescent mi-croparticles".

Author Contributions: Conceptualization, M.N.-E.-A.; methodology, M.N.-E.-A., M.V. and K.A.; software, M.N.-E.-A., M.V. and K.A.; validation, M.N.-E.-A., M.V. and K.A.; formal analysis, M.N.-E.-A., M.V. and K.A.; investigation, M.N.-E.-A. and M.V.; resources, M.N.-E.-A., M.V. and K.A.; data curation, M.N.-E.-A., M.V. and K.A.; writing—original draft preparation, M.N.-E.-A.; writing—review and editing, M.N.-E.-A. and M.V.; visualization, M.N.-E.-A., M.V. and K.A.; supervision, M.V. and K.A.; project administration, K.A.; funding acquisition, M.N.-E.-A., M.V. and K.A. All authors have read and agreed to the published version of the manuscript.

Funding: This research received no external funding.

Institutional Review Board Statement: Not applicable.

Informed Consent Statement: Not applicable.

Data Availability Statement: Not applicable.

Acknowledgments: We would like to acknowledge the academic support of School of Science, Edith Cowan University, Australia. We would also like to acknowledge our international research collaborators from the Russian Federation, Germany, Switzerland, and India.

Conflicts of Interest: The authors declare no conflict of interest.

Appendix A

The appendix contains a list of publications made by our group that related to the study of synthesis and development of various garnet materials towards their practical applications but are not cited in this article. This list will be useful for the readers, the scientific community, and the government and commercial industries.

1. YIG: Bi_2O_3 nanocomposite thin films for magneto-optic and microwave applications. *Journal of nanomaterials*, 2015, Article ID 182691, https://doi.org/10.1155/2015/182691.
2. Synthesis, characteristics and material properties dataset of Bi:DyIG-oxide garnet type nanocomposites. *Journal of nanomaterials*, 2015, Article ID 127498, https://doi.org/10.1155/2015/127498.
3. Growth, characterization, and properties of $Bi_{1.8}Lu_{1.2}Fe_{3.6}Al_{1.4}O_{12}$ garnet films prepared using two different substrate temperatures. *Int. J. Materials Engineering Innovation*, Vol. 5, No. 3, 2014, https://doi.org/10.1504/IJMATEI.2014.064275.
4. Physical properties and behaviour of highly Bi-substituted magneto-optic garnets for applications in integrated optics and photonics. *Advances in Optical Technologies*, volume 2011, Article ID 971267, 7 pages, https://doi:10.1155/2011/971267.
5. Nano-structured magnetic photonic crystals for magneto-optic polarization controllers at the communication-band wavelengths. *Opt. Quant. Electron*. 41, 661-669, 2009.
6. Analysis, optimization, and characterization of magnetic photonic crystal structures and thin-film material layers. *Technologies*, 2019, 7 (3), 49, https://doi.org/10.3390/technologies7030049.
7. Sensing of surface and bulk refractive index using magnetophotonic crystal with hybrid magneto-optical response. *Sensors*, 2021, 21, 1984.
8. Magneto-optic properties of ultrathin nanocrystalline ferrite garnet films in the 8K to 300K temperature interval. *Journal of nanomaterials*, 2018, Article ID 7605620, https://doi.org/10.1155/2018/7605620.
9. Properties of magnetic photonic crystals in the visible spectral region and their performance limitations. *Photonics and Nanostructures - Fundamentals and Applications*, 2018, Vol. 28, pp 12-19, https://doi.org/10.1016/j.photonics.2017.11.003.
10. High-Q surface modes in photonic crystal/iron garnet film heterostructures for sensor applications. *JETP Letters*, 2016, Vol. 104, No. 10, pp. 679–684, https://doi.org/10.1134/S0021364016220094.
11. Transverse magnetic field impact on waveguide modes of photonic crystals. *Optics Latter*, 2016, Vol. 41 (16), pp 3813-3816, https://doi.org/10.1364/OL.41.003813.
12. Tunable optical nanocavity of iron-garnet with a buried metal layer. *Materials*, 2015, 8(6), 3012-3023; https://doi.org/10.3390/ma8063012.
13. Magneto-optic properties of ultrathin bismuth-substituted ferrite garnet films obtained by RF magnetron sputtering method. *J. Comm. Tech. Electron.*, 2014, https://doi.org/10.1134/S1064226914110096.
14. Magneto-Photonic intensity effects in hybrid metal-dielectric structures. *Physical Review B*, 89, 045118 (2014), https://doi.org/10.1103/PhysRevB.89.045118.
15. Plasmon mediated magneto-optical transparency. *Nature Communications*, 4:2128, https://doi.org/10.1038/ncomms3128 (2013).
16. Tuning of the transverse magneto-optical Kerr effect in magneto-plasmonic crystals. *New J. Phys.*, 15, 075024, (2013), https://doi.org/10.1088/1367-2630/15/7/075024.
17. Magnetic heterostructures with low coercivity for high-performance magneto-optic devices. *J. Phys. D: Appl. Phys.*, 46 035001, (2013), https://doi.org/10.1088/0022-3727/46/3/035001. Impact Factor-2.829, Cite Score-2.75.

References

1. Zvezdin, A.K.; Kotov, V.A. *Modern Magnetooptics and Magnetooptical Materials*; Institute of Physics Publishing: Bristol, UK; Philadelphia, PA, USA, 1997; ISBN 075030362X.
2. Hansteen, F. Ultrafast Optical Control of Magnetization in Ferrimagnetic Garnets. Ph.D. Thesis, Radboud University Nijmegen, Nijmegen, The Netherlands, 2006. Available online: http://www.hansteen.net/thesis.pdf (accessed on 22 June 2022).

3. Bi, L.; Hu, J.; Jiang, P.; Kim, H.S.; Kim, D.H.; Onbasli, M.C.; Dionne, G.F.; Ross, C.A. Magneto-Optical Thin Films for On-Chip Monolithic Integration of Non-Reciprocal Photonic Devices. *Materials* **2013**, *6*, 5094–5117. [CrossRef] [PubMed]
4. Scott, G.; Lacklison, D. Magnetooptic properties and applications of bismuth substituted iron garnets. *IEEE Trans. Magn.* **1976**, *12*, 292–311. [CrossRef]
5. Nistor, I. Development of Magnetic Field Sensors Using Bisbuth-Substituted Garnets Thin Films with In-Plane Magnetization. Ph.D. Thesis, University of Maryland, College Park, MD, USA, 2006.
6. Kang, S. Advanced Magneto-Optical Materials and Devices. Ph.D. Thesis, The Pennsylvania University, Philadelphia, PA, USA, 2007.
7. Gomi, M.; Tanida, T.; Abe, M. RF sputtering of highly Bi-susbtituted garnet films on glass substrates for magneto-optic memory. *J. Appl. Phys.* **1997**, *81*, 5653–5655.
8. Buhrer, C.F. Faraday rotation and dichroism of bismuth calcium vanadium iron garnet. *J. Appl. Phys.* **1969**, *40*, 4500–4502. [CrossRef]
9. Danish, A.W. Study on Preparation and Characterization of Bismuth Substituted Gadolinium Iron Garnet Thin Films by Metal orgaini Decomposition Method. Ph.D. Thesis, Tokyo University of Agriculture and Technology, Tokyo, Japan, 2017.
10. Deb, M.; Popova, E.; Keller, N. Different magneto-optical response of magnetic sublattices as a function of temperature in ferrimagnetic bismuth iron garnet films. *Phys. Rev. B* **2019**, *100*, 224410. [CrossRef]
11. Kahl, S. Bismuth Iron Garnet Films for Magneto-Optical Photonic Crystals. Ph.D. Thesis, Royal Institute of Technology, Stockholm, Sweden, 2004. Available online: https://www.diva-portal.org/smash/get/diva2:9551/FULLTEXT01.pdf (accessed on 11 November 2008).
12. Vasiliev, M.; Alam, M.N.-E.; Kotov, V.A.; Alameh, K.; Belotelov, V.I.; Burkov, V.I.; Zvezdin, K.A. RF magnetron sputtered $(BiDy)_3(FeGa)_5O_{12}$:Bi_2O_3 composite garnet-oxide materials possessing record magneto-optic quality in the visible spectral region. *Opt. Express* **2009**, *17*, 19519–19535. [CrossRef]
13. Alam, M. High Performance Magneto-Optic Garnet Materials for Integrated Optics and Photonics. PhD Thesis, Edith Cowan University, Joondalup, WA, Australia, 2012. Available online: https://ro.ecu.edu.au/theses/528 (accessed on 30 September 2022).
14. Yao, S.; Sato, T.; Kaneko, K.; Murai, S.; Fujita, K.; Tanaka, K. Faraday effect of bismuth iron garnet thin film prepared by mist CVD method. *Jpn. J. Appl. Phys.* **2015**, *54*, 063001. [CrossRef]
15. Liu, X.; Yang, Q.; Zhang, D.; Wu, Y.; Zhang, H. Magnetic properties of bismuth substituted yttrium iron garnet film with perpendicular magnetic anisotropy. *AIP Adv.* **2019**, *9*, 115001. [CrossRef]
16. Zanjani, S.M.; Onbasli, M.C. Thin film rare earth iron garnets with perpendicular magnetic anisotropy for spintronic applications. *AIP Adv.* **2019**, *9*, 035024. [CrossRef]
17. Eschenfelder, A. *Magnetic Bubble Technology*; Springer: New York, NY, USA, 1980.
18. Aichele, T.; Lorenz, A.; Hergt, R.; Görnert, P. Garnet layers prepared by liquid phase epitaxy for microwave and magneto-optical applications—A review. *Cryst. Res. Technol.* **2003**, *38*, 575–587. [CrossRef]
19. Abe, M.; Gomi, M. Magneto-optical recording on garnet films. *J. Mag. Mag. Mate.* **1990**, *84*, 222–228. [CrossRef]
20. Inoue, M. Magnetophotonic crystals. *Mater. Res. Soc. Symp. Proc.* **2005**, *834*, J1.1.
21. Hu, S.; Guo, Z.; Dong, L.; Deng, F.; Jiang, H.; Chen, H. Enhanced Magneto-Optical Effect in Heterostructures Composed of Epsilon-Near-Zero Materials and Truncated Photonic Crystals. *Front. Mater.* **2022**, *9*, 1–10. [CrossRef]
22. Wu, Z. Planar Magneto-Photonic and Gradient-Photonic Structures: Crystals and Metamaterials. Ph.D. Thesis, Michigan Technological University, Houghton, MI, USA, 2010. Available online: https://digitalcommons.mtu.edu/cgi/viewcontent.cgi?article=1120&context=etds (accessed on 17 August 2022).
23. Da, H.; Li, Z. Manipulating nematic liquid crystals-based magnetophotonic crystals. In *New Developments in Liquid Crystals*; Tkachenko, G., Ed.; IntechOpen: London, UK, 2009.
24. Fathi, F.; Rashidi, M.-R.; Pakchin, P.S.; Ahmadi-Kandjani, S.; Nikniazi, A. Photonic crystal based biosensors: Emerging inverse opals for biomarker detection. *Talanta* **2020**, *221*, 121615. [CrossRef] [PubMed]
25. Sohlstrom, H. Fibre Optic Magnetic Field Sensors Utilizing Iron Garnet Materials. Ph.D. Thesis, School of Electrical Engineering, Royal Institute of Technology, Stockholm, Sweden, 1993.
26. Jha, A.R. *Rare Earth Materials: Properties and Applications*; CRC Press: Boca Raton, FL, USA; Taylor & Francis group: London, Uk, 2014; Available online: https://ftp.idu.ac.id/wp-content/uploads/ebook/tdg/BUKU%20REE/Rare%20Earth%20Materials%20Properties%20and%20Applications%20by%20Jha,%20A.R.%20(z-lib.org).pdf (accessed on 19 August 2022).
27. Mitra, A. Structural and Magnetic Properties of YIG Thin Films and Interfacial Origin of Magnetisation Suppression. Ph.D. Thesis, University of Leeds, Leeds, UK, 2017. Available online: https://etheses.whiterose.ac.uk/18696/1/Arpita%20Mitra_FinalThesis.pdf (accessed on 19 August 2022).
28. Zhukov, A.; Inoue, M.; Phan, M.-H.; Shavrov, V. Advanced Magnetic Materials. *Phys. Res. Int.* **2012**, *2012*, 385396. [CrossRef]
29. Urakawa, R.; Asano, W.; Nishikawa, M.; Kawahara, M.; Nishi, T.; Oshima, D.; Kato, T.; Ishibashi, T. Magneto-optical property and magnetic anisotropy of (100) oriented $R_{0.5}Bi_{2.5}Fe_5O_{12}$ (R = Eu, Sm, and Pr) thin films prepared by metal–organic decomposition. *AIP Advances* **2022**, *12*, 095322. [CrossRef]
30. Jesenska, E.; Yoshida, T.; Shinozaki, K.; Ishibashi, T.; Beran, L.; Zahradnik, M.; Antos, R.; Kučera, M.; Veis, M. Optical and magneto-optical properties of Bi substituted yttrium iron garnets prepared by metal organic decomposition. *Opt. Mater. Express* **2016**, *6*, 1986–1997. [CrossRef]

31. Alam, M.N.-E.; Vasiliev, M.; Alameh, K. $Bi_3Fe_5O_{12}$: Dy_2O_3 composite thin film materials for magneto-photonics and magneto-plasmonics. *Opt. Mater. Express* **2014**, *4*, 1866–1875. [CrossRef]
32. Nur-E-Alam, M.; Vasiliev, M.; Kotov, V.A.; Balabanov, D.; Akimov, I.; Alameh, K. Properties of Exchange Coupled All-garnet Magneto-Optic Thin Film Multilayer Structures. *Materials* **2015**, *8*, 1976–1992. [CrossRef]
33. Kotov, V.; Nur-E-Alam, M.; Vasiliev, M.; Alameh, K.; Balabanov, D.; Burkov, V. Enhanced Magneto-Optic Properties in Sputtered Bi- Containing Ferrite Garnet Thin Films Fabricated Using Oxygen Plasma Treatment and Metal Oxide Protective Layers. *Materials* **2020**, *13*, 5113. [CrossRef]
34. Nur-E-Alam, M.; Vasiliev, M.; Kotov, V.; Alameh, K. Recent Developments in Magneto-optic Garnet-type Thin-film Materials Synthesis. *Procedia Eng.* **2014**, *76*, 61–73. [CrossRef]
35. Nur-E-Alam, M.; Vasiliev, M.; Kotov, V.A.; Alameh, K. Highly bismuth-substituted, record-performance magneto-optic garnet materials with low coercivity for applications in integrated optics, photonic crystals, imaging and sensing. *Opt. Mater. Express* **2011**, *1*, 413–427. [CrossRef]
36. Nur-E-Alam, M.; Vasiliev, M.; Belotelov, V.; Alameh, K. Properties of Ferrite Garnet (Bi, Lu, Y)3(Fe, Ga)5O12 Thin Film Materials Prepared by RF Magnetron Sputtering. *Nanomaterials* **2018**, *8*, 355. [CrossRef] [PubMed]
37. Nur-E-Alam, M.; Vasiliev, M.; Alameh, K. High-performance RF-sputtered Bi-substituted iron garnet thin films with almost in-plane magnetization. *Opt. Mater. Express* **2017**, *7*, 676. [CrossRef]
38. Nur-E-Alam, M.; Vasiliev, M.; Alameh, K. Influence of Substrate Stage Temperature and Rotation Rate on the Magneto-Optical Quality of RF-Sputtered Bi2.1Dy0.9Fe3.9Ga1.1O12 Garnet Thin Films. *Appl. Sci.* **2018**, *8*, 456. [CrossRef]
39. Pankhurst, Q.A.; Connolly, J.; Jones, S.K.; Dobson, J. Applications of magnetic nanoparticles in biomedicine. *J. Phys. D Appl. Phys.* **2003**, *36*, R167–R181. [CrossRef]
40. Vasiliev, M.; Nur-E.-Alam, M.; Alameh, K.; Premchander, P.; Lee, Y.T.; Kotov, V.A.; Lee, Y.P. Annealing behaviour and crystal structure of RF-sputtered Bi-substituted dysprosium iron-garnet films having excess co-sputtered Bi-oxide content. *J. Phys. D Appl. Phys.* **2011**, *44*, 075002. [CrossRef]
41. Nur-E-Alam, M.; Vasiliev, M.; Alameh, K.; Kotov, V. Synthesis of high-performance magnetic garnet materials and garnet-bismuth oxide nanocomposites using physical vapor deposition followed by high-temperature crystallization. *Pure Appl. Chem.* **2011**, *83*, 1971–1980. [CrossRef]
42. Nur-E-Alam, M.; Vasiliev, M.; Alameh, K. Optical constants of rare-earth substituted amorphous oxide-mix-based layers deposited to enable synthesis of magneto-optic garnets. *Opt. Mater.* **2019**, *98*, 109309. [CrossRef]
43. Fakhrul, T.; Tazlaru, S.; Khurana, B.; Beran, L.; Bauer, J.; Vančík, M.; Marchese, A.; Tsotsos, E.; Kučera, M.; Zhang, Y.; et al. High Figure of Merit Magneto-Optical Ce- and Bi-Substituted Terbium Iron Garnet Films Integrated on Si. *Adv. Opt. Mater.* **2021**, *9*, 2100512. [CrossRef]
44. Voronov, A.A.; Mikhailova, T.; Borovkova, O.V.; Shaposhnikov, A.N.; Berzhansky, V.N.; Belotelov, V.I. Bismuth-Substituted Iron Garnet Films for Magnetophotonics: Part A—Fabrication Methods and Microstructure Property Study. *Inorg. Org. Thin Film.* **2021**, *1*, 125–159. [CrossRef]
45. Denysenkov, V.; Jalali-Roudsar, A.; Adachi, A.; Khartsev, S.; Grishin, A.; Okuda, T. Ferromagnetic resonancein single crystal bismuth iron garnet film. *MRS Online Proc. Libr.* **1999**, *603*, 107–112. [CrossRef]
46. Berzhansky, V.N.; Shaposhnikove, A.N.; Karavanikov, A.V.; Propkopov, A.R.; Mikhailova, T.V.; Kharchenkov, N.F.; Lukienko, I.N.; Karchenko, Y.N.; Miloslavskaya, O.V.; Kotov, V.A.; et al. The effect of Faraday rotation enhancement in nanolayered structures of Bi-substituted iron garnets. *Solid State Phenom.* **2013**, *200*, 233–238. [CrossRef]
47. Vertruyen, B.; Cloots, R.; Abell, J.S.; Jackson, T.J.; da Silva, R.; Popova, E.; Keller, N. Curie temperature, exchange integrals, and magneto-optical properties in off-stoichiometric bismuth iron garnet epitaxial films. *Phys. Rev. B* **2008**, *78*, 094429. [CrossRef]
48. Kang, S.; Yin, S.; Adyam, V.; Li, Q.; Zhu, Y. $Bi_3Fe_4Ga_1O_{12}$ Garnet Properties and Its Application to Ultrafast Switching in the Visible Spectrum. *IEEE Trans. Magn.* **2007**, *43*, 3656–3660. [CrossRef]
49. Nachimutu, R.K. Synthesis and Characterization of Cerium Substituted Iron Garnets on Amorphous Substrates. Ph.D. Thesis, The University of Western Australia, Crawley, WA, Australia, 2016.
50. Lou, G.; Kato, T.; Iwata, S.; Ishibashi, T. Magneto-optical properties and magnetic anisotropy of $Nd_{0.5}Bi_{2.5}Fe_{5-y}Ga_yO_{12}$ thin films on glass substrates. *Opt. Mater. Express* **2017**, *7*, 2248. [CrossRef]
51. Siao, Y.-J.; Qi, X.; Lin, C.-R.; Huang, J.-C. Dielectric relaxation and magnetic behavior of bismuth-substituted yttrium iron garnet. *J. Appl. Phys.* **2011**, *109*, 07A508. [CrossRef]
52. Sahoo, M.R.; Barik, A.; Kuila, S.; Tiwary, S.; Ghosh, R.; Babu, P.D.; Kaushik, S.D.; Vishwakarma, P.N. Magnetic and electrical transportstudies of polycrystallineSr1−xBixFe12O19 (x = 0, 0.01, and 0.02). *J. Phys. D Appl. Phys.* **2022**, *55*, 265001. [CrossRef]
53. Manda, C.S.; Singh, M.R. Fabrication and characterization of Bismuth-Cerium composite iron garnet epitaxial films for magneto optical applications. *J. Appl. Phys.* **2012**, *112*, 083525.
54. Botas, A.M.P. New Frontiers in Novel Optical Materials and Devices. *Coatings* **2022**, *12*, 856. [CrossRef]
55. Kimel, A.; Zvezdin, A.; Sangeeta, S.; Shallcross, S.; de Sousa, N.; García-Martín, A.; Salvan, G.; Hamrle, J.; Stejskal, O.; McCord, J.; et al. The 2022 Magneto-Optics Roadmap. *J. Phys. D Appl. Phys.* **2022**, *55*, 463003. [CrossRef]